Available online at www.sciencedirect.com

SCIENCE DIRECT®

Sedimentary Geology 168 (2004) 227–247

Sedimentary Geology

www.elsevier.com/locate/sedgeo

Early post-impact sedimentation around the central high of the Mjølnir impact crater (Barents Sea, Late Jurassic)

Henning Dypvik[a,*], Pål T. Sandbakken[b], George Postma[c], Atle Mørk[d]

[a] *Department of Geosciences, University of Oslo, P.O. Box 1047, Blindern, N-0316 Oslo, Norway*
[b] *Statoil ASA, UPN TO SF, RESU-SFC, B4, FV, N-4035 Stavanger, Norway*
[c] *Faculty of Earth Sciences, Utrecht University, P.O. Box 80021, 3508 TA, Utrecht, The Netherlands*
[d] *SINTEF Petroleum Research, N-7465 Trondheim, Norway*

Received 11 June 2003; received in revised form 6 January 2004; accepted 18 March 2004

Abstract

The Mjølnir bolide created the 40-km diameter Mjølnir crater, when it impacted the black, mostly anoxic clays of the Hekkingen Formation in the paleo-Barents Sea about 142 ± 2.6 million years ago. The normally calm, 300–500 m deep epicontinental depositional environment was suddenly disrupted by the dramatic effect of the impact, resulting in a brief period of extreme sediment reworking and redeposition. The hypoxic to anoxic depositional conditions characteristic of the Hekkingen Formation returned to the impact site soon after the collapse, when the major modification phases of the Mjølnir crater were completed.

We have studied a shallow core (121 m long) retrieved from the flanks of the central high in the Mjølnir crater. The core shows a complex depositional succession of the Ragnarok Formation, which is related to both the uplift and the subsequent collapse and drowning of the central high. The basal part of the core consists of chaotically organised, large folded slabs of pre-impact substrate, which we infer to be related to the rapid steepening of the slope of the central high during its rising shortly after the impact. The slump deposits are overlain by a diamict, which is interpreted to originate from debris flows that originate by liquefaction and subsequent remoulding and remobilisation of sediment from the collapsing central high. The diamict is in turn covered by a brecciated, graded mudstone that records the action of impact-related tsunami and the subsequent submergence of the impact crater. A sequence of mainly debris flow and turbidite deposits separates the impact-related deposit from the overlying shelf sediments of the Hekkingen Formation and forms the last post-impact sedimentary recorder of the presence of a central high in the crater.

Keywords: Marine impact; Crater fill; Slump; Mass flow; Turbidite; Tsunami

1. Introduction

1.1. Background and study objectives

In 1998, the Mjølnir core (7329/03-U-01) was drilled in order to study both syn-impact and post-

* Corresponding author. Tel.: +47-22-85-66-59; fax: +47-22-85-42-15.
E-mail addresses: henning.dypvik@geologi.uio.no (H. Dypvik), ptrsa@statoil.com (P.T. Sandbakken), gpostma@geo.uu.nl (G. Postma), atle.mork@iku.sintef.no (A. Mørk).

0037-0738/$ - see front matter © 2004 Elsevier B.V. All rights reserved.
doi:10.1016/j.sedgeo.2004.03.009

impact sedimentation of the Mjølnir impact crater (Gudlaugsson, 1993; Dypvik et al., 1996). The aim was to shed light on the mechanisms of formation and sedimentation of the Mjølnir impact crater and its surroundings. We aimed at getting more general information on the processes of marine impacts and the early post-impact processes of crater sedimentation. These processes are poorly known in this relatively young field of research and have been discussed only in studies of the Chesapeake Bay (Poag et al., 2002, 2003), Montagnais (Jansa et al., 1989) and Lockne craters (Lindstrøm et al., 1996; Von Dalwigk and Ormø, 2001). Because the Mjølnir crater is one of the most thoroughly studied and described marine impact structures, core 7329/03-U-01 is well suited for this purpose.

Impacts of asteroids and comets are quite common in geological history, and can be recognized by specific physical and chemical characteristics (Melosh, 1989). However, sedimentary features related to the syn- and early post-impact deposition need to be explored in more detail for the results to be useful for recognition of impact events elsewhere in the rock record. Numerical modeling results (Shuvalov et al., 2002; Shuvalov and Dypvik, in press) show the development of the marine Mjølnir impact crater in conjunction with rebound and rise of a central high. In marine craters, the central high may form a temporary island in shallow seas, before collapse of the island and the crater rim contribute to the infill of the crater (Dypvik and Jansa, 2003). Consequently, the sediments of submarine impact craters differ significantly from those of subaerial impact craters, because sediment transport is controlled by the collapse of water-saturated and unstable sediments, tsunami generated waves and currents, and by later subaqueous reworking of the crater rim and the flanks of the central high. Hence, sediments in cores from within a marine crater can be expected to be highly influenced by *en-masse* sediment sliding and slumping and by sediment gravity flows.

Numerical models used to simulate the Mjølnir impact indicate that the parautochtonous rocks of the central high should be overlain by allochtonous sediments derived to a large degree from collapse and slumping from the central high (Shuvalov et al., 2002; Shuvalov and Dypvik, in press). In the case of the Chesapeake Bay (Poag et al., 2002, 2003) and the Montagnais (Jansa et al., 1989) impact craters, allochtonous crater-fill breccias bury the peak rings and the central highs. More than 160 m of such sediments are found in the case of the Montagnais crater. Jansa et al. (1989) suggested that the occurrences of thick breccia sequences capping the central high might be a characteristic of marine impact craters, since this had not yet been observed in subaerial impacts.

This paper presents the first detailed descriptions of the 121-m long Mjølnir core (7329/03-U-01). The core contains the sediments from the flank of the central high, and as such, gives insight into the sequence of events that occurs shortly after a submarine impact.

1.2. The Mjølnir crater

The Mjølnir crater is located in the Barents Sea below about 50–150 m of post-Jurassic sediments and 350 m of water (Fig. 1). Its presence was first discovered by geophysical surveys (Gudlaugsson, 1993), but cores from nearby drill holes in the Barents Sea provided further evidence for its impact origin (Dypvik et al., 1996; Sandbakken, 2002).

The Mjølnir crater was formed by an asteroid impact in the paleo-Barents Sea probably in early Berriasian time (i.e. Ryazanian, Late Jurassic/Early Cretaceous, the *Berriasiella jacobi* zone (142 ± 2.6 Myr) (Dypvik et al., 1996; Smelror et al., 2001a,b). The wide Berriasian epicontinental sea with 300–500 m water depth was populated by a rich fauna and flora (e.g. bivalves, belemnites, ammonites, plesiosaurs are commonly found). The depositional conditions in the paleo-Barents Sea were dominated by hypoxic (0.2–2.0 ml O_2/l H_2O) to anoxic bottom environments with predominantly accumulation of dark, organic-rich clays (Worsley et al., 1988; Smelror et al., 1998; Leith et al., 1993).

After impact, the Mjølnir structure evolved through an initially (transient) 16-km crater diameter to a 40-km wide crater (final stage), containing a central peak (basal diameter of 8 km), and an annular basin (12 km in diameter) (Fig. 1; Tsikalas et al., 1998a,b,c). The development of the final 40-km wide crater was initially a result of crater modification, resulting in rim and central high collapse and sedimentation. Originally much material was ejected (estimated to

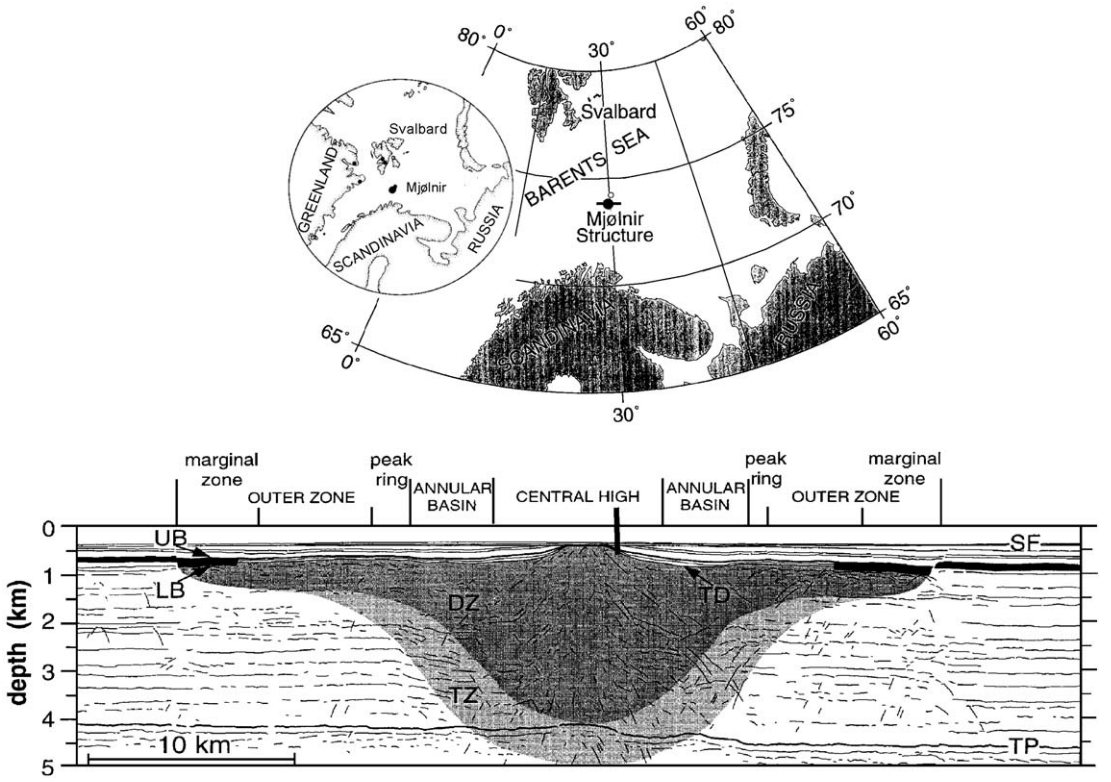

Fig. 1. Geographical and paleogeographical (Late Jurassic) (circular) position of the Mjølnir crater. The lower part shows an interpreted W–E seismic section across the structure, along the line on the geographical map (modified from Dypvik et al., 1996). UB = upper Barremian, LB = lower Barremian, TP = top Permian, SF = sea floor.

be in the order of 230 km^3; Shuvalov et al., 2002) from the transient crater, with a relatively small amount of material transported back into the crater during the collapse and the modification phase. The coarse debris was deposited around the crater, whereas fine grained ejecta was widely transported outside the crater (Shuvalov and Dypvik, in press). Ejecta has been found in cores for example from elsewhere in the Barents Sea and in outcrops on Svalbard (Dypvik et al., 2000). Ejecta also may be present in the sedimentary succession of Nordvik in central Siberia (Zakharov et al., 1993).

Numerical simulations of the Mjølnir impact generated by Shuvalov et al. (2002) show that a mega-tsunami formed shortly after the time of impact. The simulations also indicate that the central high may have been more than one km high and that the tranquil pre-impact conditions where not re-established until at least 20 min after impact (Shuvalov et al., 2002). Local depositional environments most likely took a much longer time to re-establish into pre-impact Hekkingen conditions and the central high may have formed an island in the paleo-Barents Sea.

2. Results—7329/03-U-01 core description

The Mjølnir core is 54 mm in diameter and was drilled in August 1998, by the drill-ship M/S Bucentaur, with IKU/SINTEF Petroleum Research as operator. The 7329/03-U-01 borehole is 171 m deep, but did not sample the upper 50 m of Quaternary sediments. The lower 121 m was cored with a recovery of 99%. The cored section comprises reworked Triassic and Jurassic sediments remobilised during impact and in situ Lower Cretaceous beds. A detailed presentation of the stratigraphical and micropaleontological char-

acterization of the different units is in preparation (Dypvik et al., pers. comm.).

The lowermost part of the core (171–74.05 m) contains impact related sediments of the Ragnarok Formation (Figs. 2 and 3), and the upper part of the core (74.05–57.2 m) contains the typical dark-grey to black mudstones of the Hekkingen Formation (Worsley et al., 1988) and the light greenish, grey marls (57.2–50.1 m) of the Klippfisk Formation (Smelror et al., 1998). The Ragnarok Formation can be separated into two units: unit I (171–88.35 m) contains plastically deformed and fractured slabs of the original Triassic to Late Jurassic substratum and unit II (88.35–74.05 m) comprises a succession of diamicts, conglomerates, sandstones, mudstone and mudstone-breccias.

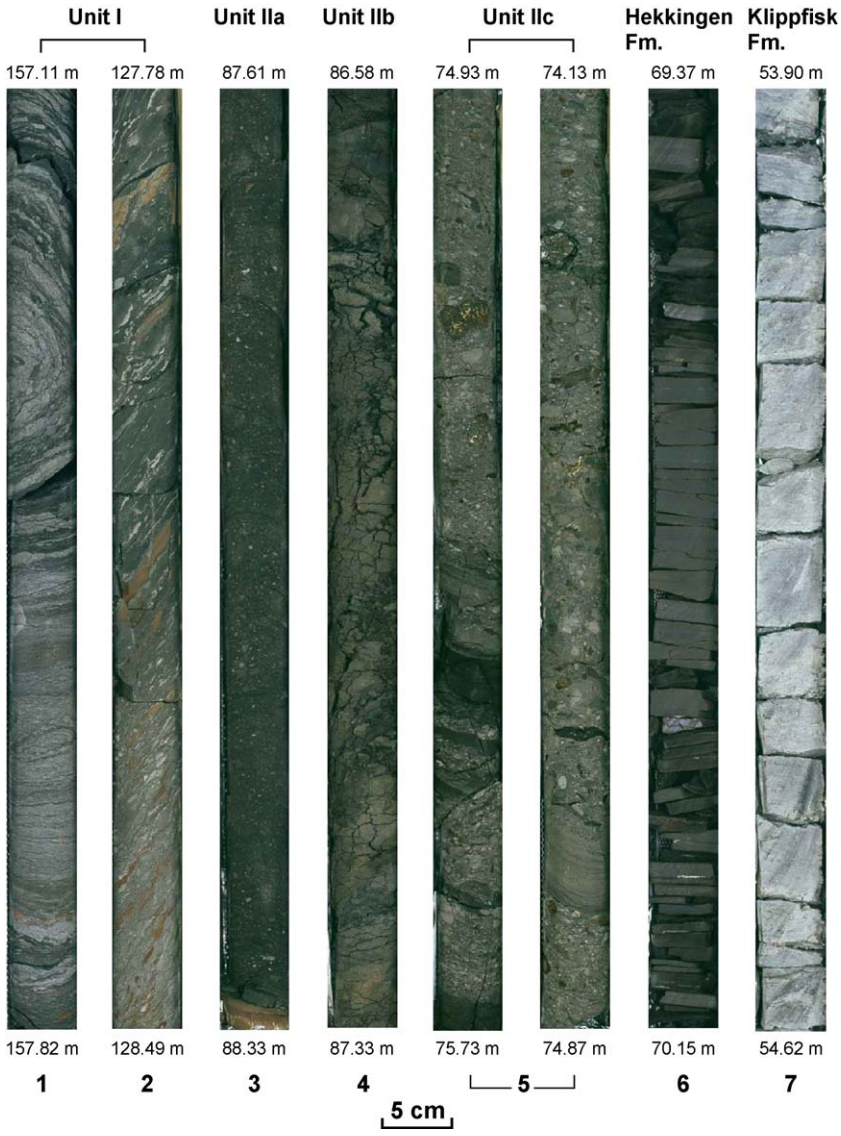

Fig. 2. An overview of the major stratigraphical units in core 7329/03-U-01. Details in Figs. 4–12.

2.1. The Ragnarok Formation

2.1.1. Unit I

Unit I (171–88.35 m) consists of strongly folded and fractured subunits of original Upper Triassic to Middle Jurassic clay-, silt- and sandstones. The degree of folding and fracturing is unevenly distributed throughout the core and in some parts both vertical and horizontal bedding are found (Figs. 2–4), often in combination with soft-sediment deformation (folding) and fluid escape structures.

The subunits have characteristic lithological and structural composition (Figs. 3 and 4). In the lower 13 m of the core (171–158.0 m), the internal bedding dips 45°. The lowermost 7.5 m are composed of dark brown claystones/shales with lighter coloured bands of siltstones, whereas the overlying 5.5 m are dominated by inter-bedded sand- and siltstones. Massive, light grey, well-sorted sandstones dominate in the interval from 158.0 to 148.0 m; these sandstones are relatively homogeneous, except for some soft-sediment deformation structures. This section grades into a dark-grey mudstone-dominated section (142.3–139.1 m), which contains homogeneous claystones with bands of silt- and sandstone. Alternating sandstone- and mudstone-dominated subunits are found in the upper part of unit I, all with diverse types of chaotic bedding.

The uppermost 120 cm of unit I contains a diamict (level 89.55–88.35 m) (Fig. 4), which is in sharp contact with an overlying siderite layer of subunit IIa (Fig. 5). The diamict is monomict, mainly clast-supported, and contains folded mud clasts (Fig. 4). Clast composition is dominated by grey mudstone with a low content of silt and sand similar to the lithology of the underlying sedimentary unit.

The mudstones in the subunits of unit I contain 90–95% clay-sized material, while the sandstones contain from 35% to 50% up to 80% sand. The sand grains are subangular to angular, mainly composed of quartz and plagioclase. The well-sorted sandstones are often cemented by chert and carbonates.

2.1.2. Unit II

Unit II (88.35–74.05 m) is divided into three subunits (Fig. 3): subunits IIa, IIb and IIc (Figs. 3–10; Table 1) each representing quite different depositional characteristics. Unit IIa is a typical diamict, unit IIb is a brecciated mudstone and unit IIc consists of a variety of conglomerate, sandstone and mudstone beds. The sediments of unit II are poorly cemented and disintegrates easily in water.

2.1.2.1. Subunit IIa. At the base of unit II, a light brown, dense siderite bed 5 cm thick (88.35–88.30 m) (Fig. 5) occurs. It has septarian cracks in its lower 3.5 cm. This part is also lighter coloured than the upper 1.5 cm, which shows a faint, parallel lamination. The horizontal orientation may indicate that the cored siderite is part of a siderite bed and not a transported concretion.

The major part of subunit IIa is a 87-cm-thick (88.30–87.43 m) diamict, with a dark-grey, silty to sandy mudstone matrix and angular litho-fragments up to about 2 cm in length, with 2 mm average grain size (Figs. 3 and 5, Table 1). It sharply overlies the siderite. The diamict is poorly sorted and structureless, apart from its faint, thinly layered structure and few intercalated centimeter-thick mudstone layers with faint irregular laminae. It is tempting to subdivide the diamict into a number of beds on basis of these mudstone partings, yet it remains unclear if there is a real physical discontinuity here. It is possible that the mudstone layers and the irregular lamina represent shear zones (see further the discussion chapter). The level between (88.10–87.70 m) shows more lightly coloured, sub-rounded fragments, especially in the upper part (87.85–87.70 m). The latter layer may reflect an additional input from a different source lithology, but presently we do not have any good candidates. At level 87.70–87.43 m, there is some clast enrichment in its uppermost part and faint increase in clast size.

The lithological composition of the clasts resembles those of the remobilised Triassic–Jurassic sediments found in unit I (Fig. 5). In thin section, the litho-fragments are seen to make up 30–40% of the rock. They float in a dark brown, sandy mud and are in some levels horizontally bedded. The amount of sand is less than 10% of the matrix volume and composed of fine to medium-sized, subangular to angular grain of mainly quartz and plagioclase composition. The fragments are composed of silty and micaceous mudstone and pure claystone. They are only slightly plastically deformed. A few minor (about 0.7 mm) siltstone fragments are also present, but no

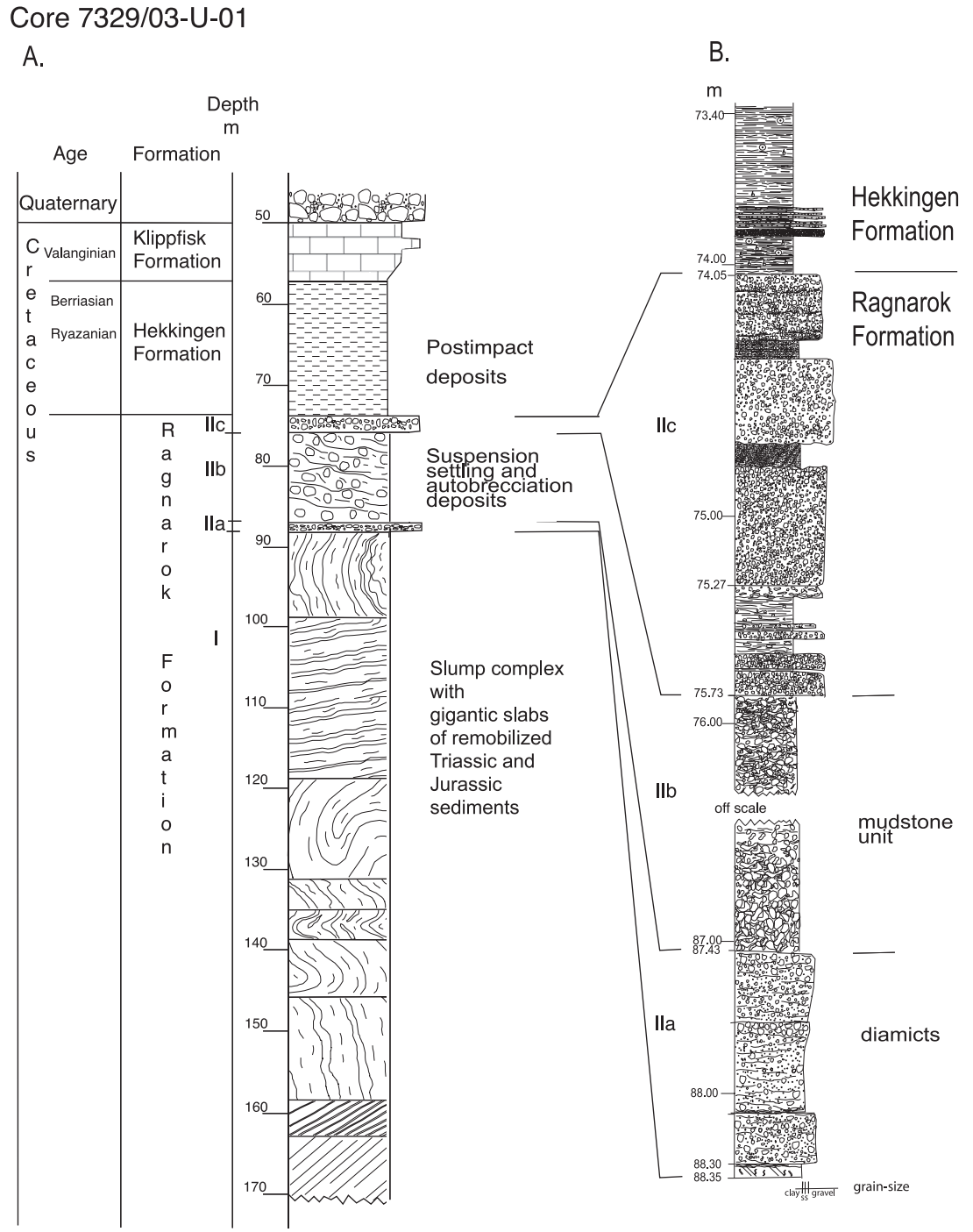

Fig. 3. An overview-log of core 7329/03-U-01 (A) and unit II of the Ragnarok Formation and the lower part of the Hekkingen Formation (B).

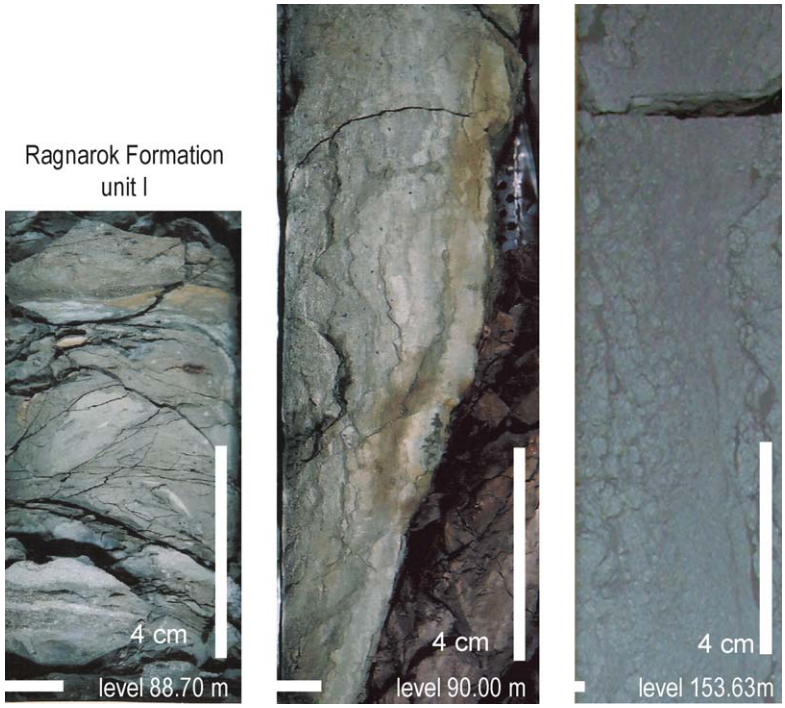

Fig. 4. Photographs of unit I (core 7329/03-U-01). The core piece from level 88.70 m illustrates the brecciated top of unit I. At level 90.00 m, a folded slab with vertical standing bedding. At level 153.63 m, an example of a fluid escape structure is found.

melt/glass or melt/glass—fragments have been found. In the upper part of subunit IIa, specimens of the same algal genus *Leiospheridia* are present, as in the overlying Hekkingen Formation (see further below).

2.1.2.2. Subunit IIb

Macroscopically subunit IIb (87.43–75.73 m) is a 11.70-m-thick, structureless, upward graded (Table 2) unit, which consists of dark-grey to brown and olive-green mudstone (Figs. 6 and 7), without internal bedding apart from a faintly laminated, clast-free interval between 84 and 81 m. Locally (e.g. 79.40 m), chemical alteration structures are seen as somewhat lighter bands crossing the core. Brownish alteration bands and spots are found sporadically. These are most likely secondary diagenetic features. A few centimeter-sized siderite concretions also occur.

Microscopically, subunit IIb can be seen to consist of a clast-supported mudstone breccia with mudstone matrix. The fragments have a similar composition to the matrix, containing about 10–20% silt and virtually no sand, and seem to have moved very little relative to each other (jigsaw puzzle type fabric). The fragments range in size from ~4–5 mm (up to 7 mm) in the lower 4–5 m of the unit (samples 87.20–83.00 m) to ~1.5–2 mm (up to 3 mm) in the upper part (82.5–75.81 m) of the unit. The clasts are angular to subangular. They show internal mechanical deformation, and a few of them show folding of original laminae. In between the brecciated parts is a 1–2-m-thick interval of apparently homogenous mud. Pyrite is seen throughout the unit as small, framboidal aggregates, either finely dispersed or in larger nodules.

In the uppermost 2.5 m of subunit IIb specimens of the algae *Tasmanites* (Fig. 7) (Bremer et al., 2003) are found together with 1–3-cm sized pyrite concretions. The *Tasmanites* are seen usually as about 0.5 mm flattened spheres of black, organic matter, with a well-defined orange to green appearance in thin sections. Similar *Tasmanites* specimens are abundant in Triassic sediments on Svalbard (A. Mørk, pers. comm.) and in drillings elsewhere in the Barents Sea (Vigran et al.,

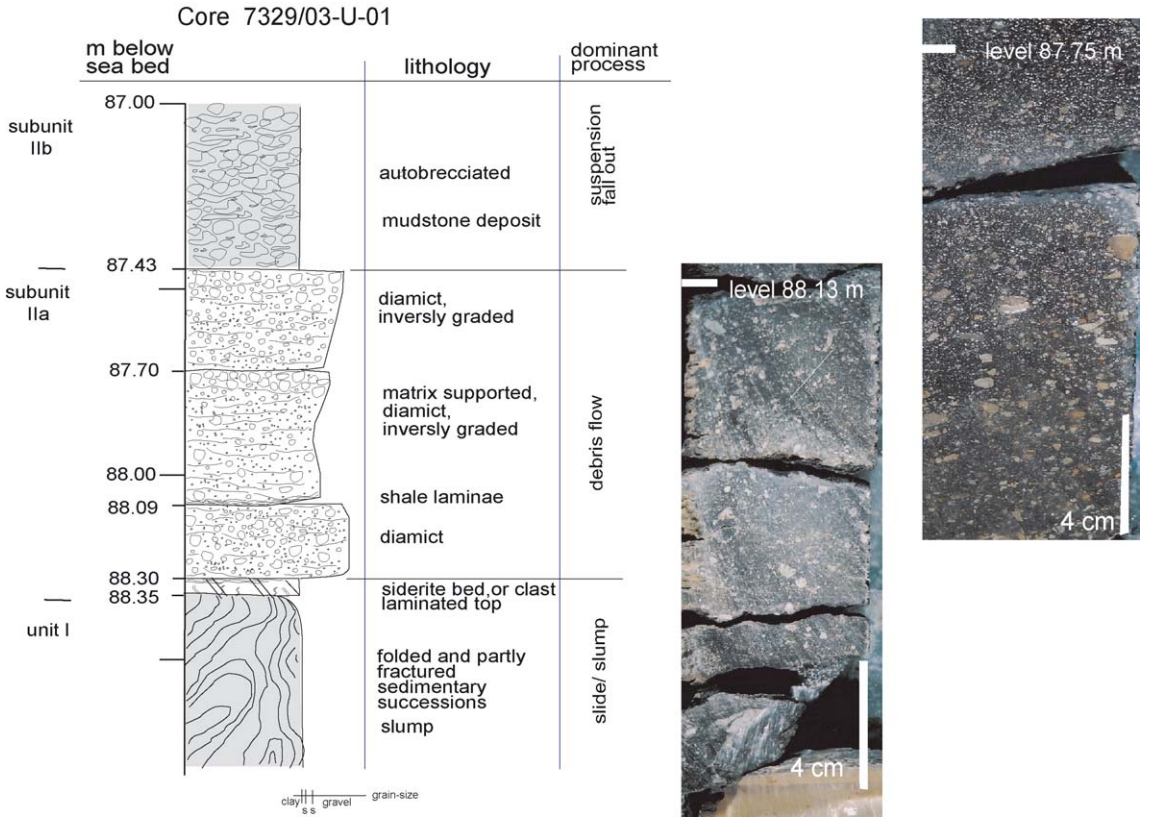

Fig. 5. Detailed log and lithological information of subunit IIa (88.35–87.43 m), the underlying unit I and the overlying subunit IIb of the Ragnarok Formation in core 7329/03-U-01. The photograph at 88.13 m illustrates the fine-grained debris flow beds of subunit IIa and the upper laminated part of the siderite bed along its base. Legend in Fig. 8. Descriptions in Table 1.

1998, pers. comm.). The contact between subunits IIb and IIc is sharp.

The analysed samples (clay fragments and matrix together) consist of more than 90% coarse clay and fine silt, with average grain sizes between 3.3 and 13.4 μm (Table 2). The results were obtained with a Malvern particle sizer Mastersizer S with a 300 mm focal length lens. In the uppermost samples, indications of bimodality are seen in the distributions, with minor enrichments in the ca. 40–50 μm grain sizes. This distribution may partly be due to the *Tasmanites* algae, whose specimens range in size from 40 μm to 2 mm. Otherwise, the grain-size distribution in subunit IIb can be characterized as unimodal and slightly fining upward.

2.1.2.3. Subunit IIc. Well-defined conglomerate beds and minor sandstone and mudstone beds are characteristic for the general light grey subunit IIc (75.73–74.05 m; Figs. 8–10; Table 1).

The three thickest conglomeratic beds (Fig. 8) are poorly sorted and clast-supported with mainly subangular to sub-rounded clasts of greyish sand, silt and mudstone composition. Rare, brown-coloured sandstone clasts show light coloured alteration rims, whereas no comparable rims have been observed on the much more common grey clasts (Fig. 10).

The structure of the lowermost conglomerate bed (75.73–75.54 m) is massive, clast-supported and contains thin, intercalated sandstone layers (Fig. 8). It is covered by a succession of very thinly, poorly bedded conglomerate, sand- and laminated dark-gray mudstone beds with outsized clasts in level (75.54–75.33 m). The laminated mudstone is sharply overlain by a 7-cm-thick (75.33–75.27 m)

Table 1
Detailed lithostratigraphical subdivision of core 7329/03-U-01

Stratigraphic unit	Depth	Lithology	Interpretation-tentative processes
Klippfisk Formation	50.00–57.20 m	Very light greenish grey marls and carbonates, fossiliferous.	Hemipelagic and pelagic rain
Hekkingen Formation	57.20–68.00 m	Light grey shales laminated, in some parts no fossils. From 63 m and up core rich in bioturbation	Hemipelagic rain
	68.00–73.78 m	Dark grey to black organic-rich shales, rich in fossils. Parallel lamination.	Hemipelagic rain
	73.78–73.89 m	Interval with conglomerates and sandstones in mudstones.	Storm-triggered turbidity currents
	73.89–74.05 m	Dark grey to black organic-rich shales, rich in fossils. Parallel lamination.	Hemipelagic rain
Subunit IIc, Ragnarok Formation	74.05–74.31 m	Matrix- and grain-supported, pebbly mudstone, faintly laminated	Mainly en-masse sediment transport possibly related to debris flow and/or turbidity current transport
	74.31–74.37 m	Parallel laminated, medium sandstones	
	74.37–74.71 m	Massive, grain-supported conglomerate	
	74.71–74.81 m	Medium sandstone, planar cross bedding, well sorted.	
	74.81–75.27 m	Clast-to matrix conglomerate, general inverse grading with faint cross bedding	
	75.27–75.33 m	Fining-upwards sandstone with clay clasts, matrix supported	
	75.33–75.42 m	Matrix-supported conglomerate, clay clasts	
	75.42–75.48 m	Matrix-supported conglomerates with thin clay beds	
	75.48–75.54 m	Mudstone with outsized clay clasts, matrix-supported	
	75.54–75.61 m	Thin clay bed overlain by a homogenous, clast-supported conglomerate	
	75.61–75.73 m	Homogenous, clast-supported conglomerate	
Subunit IIb, Ragnarok Formation	75.73–79.50 m 79.50–83.00 m 83.00–87.43 m	Dark grey to brown, olive green, normally graded mudstone. Contains levels that are in situ brecciated (jigsaw puzzle fabric).	Suspension fall-out
Subunit IIa, Ragnarok Formation	87.43–87.70 m 87.70–88.09 m 88.09–88.30 m	Matrix supported conglomerate beds	Debris flow (mud flow)
	88.35–88.30 m	Siderite bed, septarian lower part and laminated darker brown upper part	
Unit I, Ragnarok Formation	88.35–171 m	Folded and fractured bedded sandstones, siltstones and shales with a few alternating carbonate beds. 120 cm monomict breccia at top of interval.	Slumping and sliding of large sediment slabs

poorly sorted sandstone bed with clay clasts, which is succeeded by the overlying conglomeratic bed (75.27–74.81 m). The latter is structureless, clast-to matrix-supported and abruptly overlain by a 10-cm-thick, cross-laminated (~ 30°) and well-sorted sandstone (74.81–74.71 m) (Figs. 9 and 10). The cross-laminated sand is in continuity with the matrix of the underlying (middle) conglomerate, pointing to continuity in sediment source. The next conglomerate bed (74.71–74.37 m) in unit IIc truncates sharply the cross-laminated sandstone and shows an increased clast-density upwards, whereas the conglomeratic bed at level 74.31–74.05 m contains more clay matrix. A 6-cm-thick

Table 2
Bulk grain size analyses of unit IIb from core 7329/03-U-01. Grain size at 10, 50 and 90 percentile

Sample level (m)	D10 (μm)	D50 (μm)	D90 (μm)
75.98	2.30	13.40	83.20
76.53	1.40	3.30	9.00
77.77	1.50	3.80	15.90
78.50	1.70	4.20	11.30
79.05	1.80	4.30	11.20
80.00	1.80	4.90	15.30
80.73	2.00	7.40	63.70
81.62	2.20	7.40	24.20
82.13	1.80	4.50	13.30
85.18	1.90	4.80	13.00
86.10	1.90	6.00	18.30
86.42	2.30	9.30	30.00
87.02	1.80	4.60	13.30
87.33	2.00	6.60	22.50
87.36	2.20	7.30	24.30
87.41	1.80	5.50	21.90

interval of parallel-laminated sandstone (74.37–74.31 m) separates the two latter conglomerate beds. The transition to the overlying Hekkingen Formation mudstones is sharp.

In thin section, the clasts are seen to be composed predominantly of dark brown claystones and mudstones, some of them containing silt, either dispersed in the rock or in laminae (Fig. 10). There are also few clasts of very fine-grained and well-compacted sandstone, with concavo-convex grain contacts. These are composed of quartz and a minor amount of feldspars and chert, cemented by clay minerals, hematite or carbonates. Similar clasts to these were not seen in unit IIa, but similar lithologies are present in unit I. Some of the lighter grayish-brown mudstone clasts resemble those seen in unit IIa, but commonly contain less silt, while the majority of the clasts in unit IIc are darker brown in thin section, some even are very dark and have a similar color to the mudstones of the Hekkingen Formation. The matrix in the conglomerates is poorly sorted and clay-rich, fine to medium grained sand containing few *Tasmanites* algae. The amount of sand in the matrix is about 50%, composed mostly of subangular to angular quartz and plagioclase grains with a minor amount of chert grains. Some of the quartz grains in the matrix show planar microstructures and subtle planar features.

2.2. Hekkingen Formation

The Hekkingen Formation (Figs. 3, 8, 11 and 12) consists in its lower part of dark grey, organic-rich, laminated mudstones. They contain abundant specimens of *Buchia* sp., some even with their aragonite nacreous coating preserved. The formation carries abundant pyrite concretions (0.2–2 cm) and some pinkish brown siderite concretions. This is characteristic for the Hekkingen Formation, as occurring elsewhere in the Barents Sea (Worsley et al., 1988; Leith et al., 1993) (Figs. 11 and 12). In thin sections, remnants of Prasinophytae (*Leiospheridia*) algae (20–50 μm in diameter) have been observed in the lower part of the formation.

In core 7329/03-U-01, the Hekkingen Formation is present between 74.05 and 57.10 m (Figs. 2, 8, 10, 11 and 12; Table 1), and is overlain by the light greenish-grey limestones and marl of the Klippfisk Formation (Lower Cretaceous) (Smelror et al., 1998).

In the interval from 73.89 to 73.78 m (Figs. 8 and 11), six very thin conglomeratic layers occur with clast-supported textures. The lowest and thickest layer is a well-defined, 5-cm-thick conglomerate bed. It has sharp upper and lower boundaries and consist of reworked dark grey clasts of the Hekkingen Formation. The other five thin layers are made up of various lighter coloured clasts of clay-silt- and sandstones, as in the conglomerates underlying subunit IIc.

From 73.78 m to the top of the Hekkingen Formation (level 57.10 m), parallel laminated grey mudstones dominate. The lower part is enriched in *Buchia* shell fragments. The mudstones are dark grey up to about level 68 m, whereas the upper part (68–57.10 m) consists of light grey mudstones. In a zone from 65 to 63 m, no macrofossils were found, but they are again present in the upper part of the Hekkingen Formation from 63 to 57.10 m. In addition, trace fossils (*Chondrites*, *Planolites*, *Teichicnus*) and carbonate concretions are common at different levels in the upper part of the succession.

Thin section observations show that 5–20% silt is mixed with the clay, and lenses of reddish, possibly organic material are typically oriented along the lamination (Fig. 12). Pyrite is seen both finely dispersed and in concretions. Chlorite is present in rod-shaped aggregates (~ 0.05 mm). Spherical algae

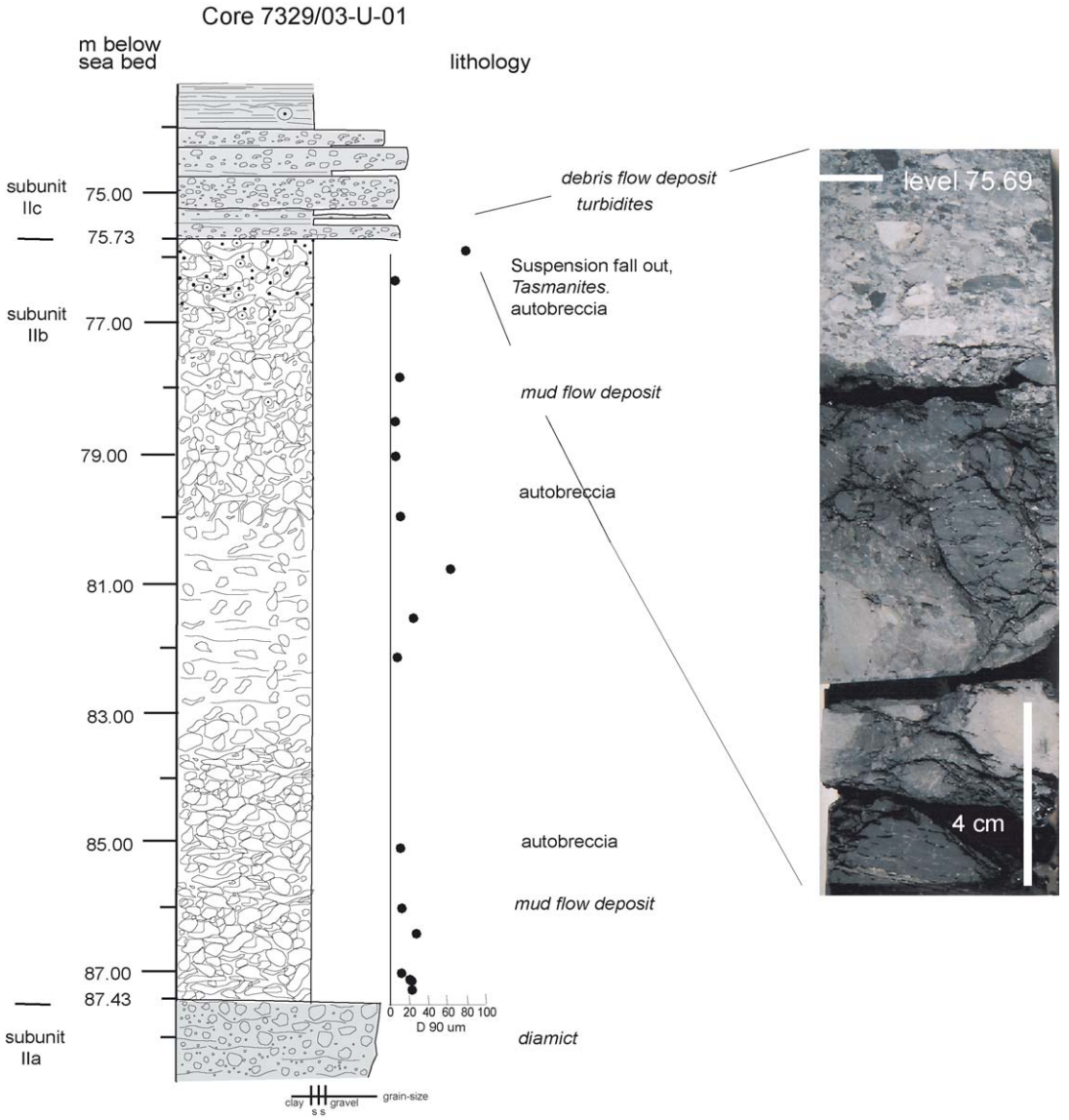

Fig. 6. Detailed log and lithological information of subunit IIb (87.43–75.73 m), the underlying subunit IIa and the overlying subunit IIc of the Ragnarok Formation. The photograph illustrates the top breccias of subunit IIb and, in the upper part (75.73–75.69 m), the lowermost conglomerate of subunit IIc. Legend in Fig. 8. Grain-size values (D90 μm) shown as black dots along subunit IIb log. Grain-size values in Table 2 and descriptions in Table 1.

(*Leiospheridia*) (Bremer et al., 2003), 25–50 μm in size, are abundant throughout the formation (Fig. 12). These algae are different in color, general appearance and size (1/10 in size) from the algae (*Tasmanites*) seen in unit IIb (Fig. 7) and are also about 1/10 in size.

3. Discussion

We discuss the occurrences of the different sediment features of the Ragnarok Formation in relation to the sequence of events in terms of post-impact reworking of the sediments derived

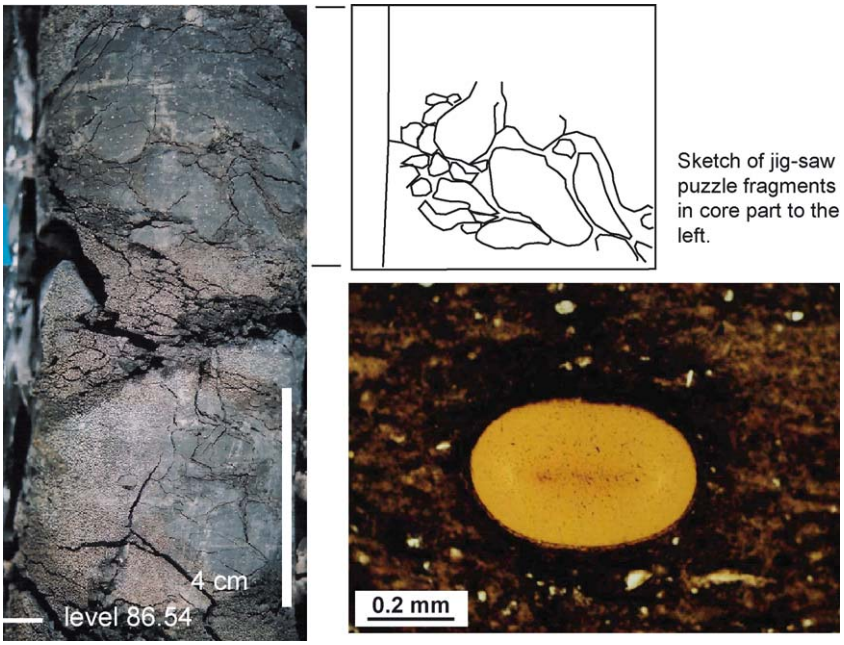

Fig. 7. The left figure illustrates the typical jigsaw puzzle conglomerates of subunit IIb (level 86.54 m), to the upper right a sketch of jigsaw puzzle part of core. To the lower right: thin section micrograph of a *Tasmanites* alga from uppermost part of unit IIb (level 76.25 m) (plane-polarized light).

from the remobilisation of the central high. Since the Mjølnir core is located high up on the central high and about 15 km from the crater rim, the cored sedimentary sequence records the impact-related events that occurred around the central high rather than the processes related to collapse of the crater rim. The black, organic-rich mudstones of the hypoxic to anoxic Hekkingen Formation, representing the Late Jurassic sea bed of an epicontinental sea (Leith et al., 1993), formed the upper few hundred meters of the pre-impact sedimentary column at the impact site.

3.1. Unit I—initial uplift and rise of the central high

The folded and fractured subunits of unit I, each with their characteristic lithologies, are inferred to represent large sediment slabs of the original substrate that were emplaced by either sliding or slumping. This is further confirmed by the sharp boundaries of the subunits and the different orientation of the internal bedding structure. The emplacement of large slabs of the original substrate is attributed to the intense uplift of the rising central high and subsequent violent sliding and slumping along the slope (Fig. 13). Some of the subunits display well-developed fracturing, much of which may be attributable to the shock waves from the impactor in concert with the central high uplift and collapse. Soft-sedimentation deformation and fluid escape structures (Fig. 4) indicate that most of the sediments were poorly consolidated at the time of impact.

At the top of unit I, the 120-cm-thick diamict, compositionally very similar to the underlying succession, is inferred to represent reworking of the top of the slide/slump deposit before the deposition of the next unit. If this is indeed the case, it marks a period where the en-masse collapsing of the rising central high was interrupted or succeeded by a stage of much more viscous (watery) debris flow. We speculate that the sliding and slumping came to a halt when the steepening of the slope stopped. Hence, the reworking of the top of this unit would mark the end of the uplift phase of the central high. It is unclear at this point if the reworking of the top

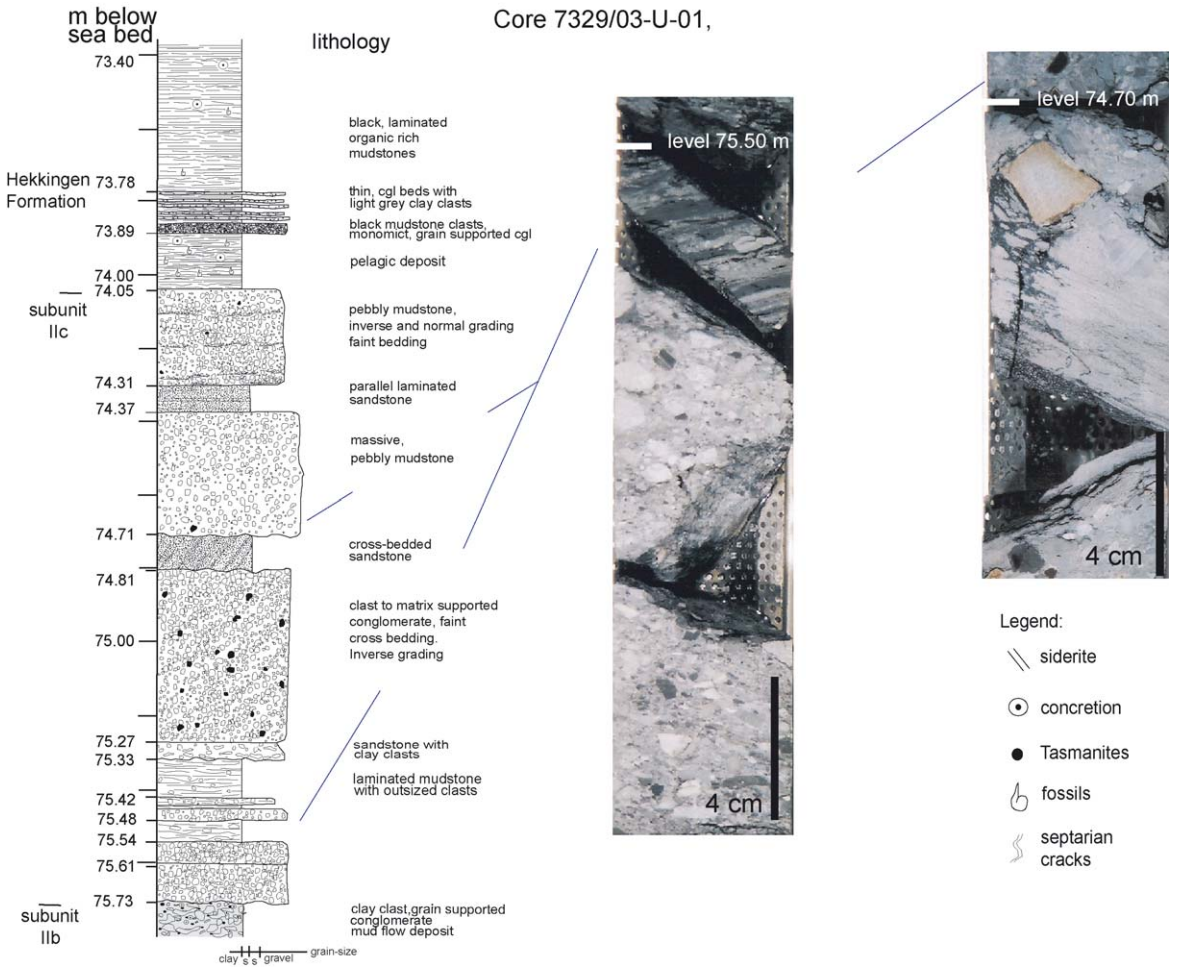

Fig. 8. Detailed log and lithological illustrations of subunit IIc (level 75.73–74.05 m) of the Ragnarok Formation and the lower part of the Hekkingen Formation, as seen in core 7329/03-U-01. The photographs illustrate the massive conglomerate bed (at level 75.50 m) and the cross-bedded sandstone at level 74.70 m), both in the Ragnarok Formation. Descriptions in Table 1.

of unit I may be ascribed to the first tsunami, or whether it is related to unstable segments of the slump deposit itself.

The sediments of unit I can reasonable be compared with the allochtonous crater-fill breccia of French (1998). It is certainly less plausible that unit I is part of uplifted par-autochthonous sedimentary rocks, since such successions, in detail, would be less modified and less mixed than the seriously disturbed sediments seen here. Hence, we infer that the flanks of central high in the crater underwent gravitational modification represented by the unit I sequence, in agreement with the numerical modelling results of Shuvalov et al. (2002). This could all have occurred subaerially, during the first few minutes of crater formation when the water masses were displaced from the impact area and the central high rose.

3.2. Unit II—crater modification and early post-impact, marine reworking of the central high

According to the simulation results of Shuvalov et al. (2002), the central high would collapse, while the water would rush back and forth within the crater for at least 20 min after impact.

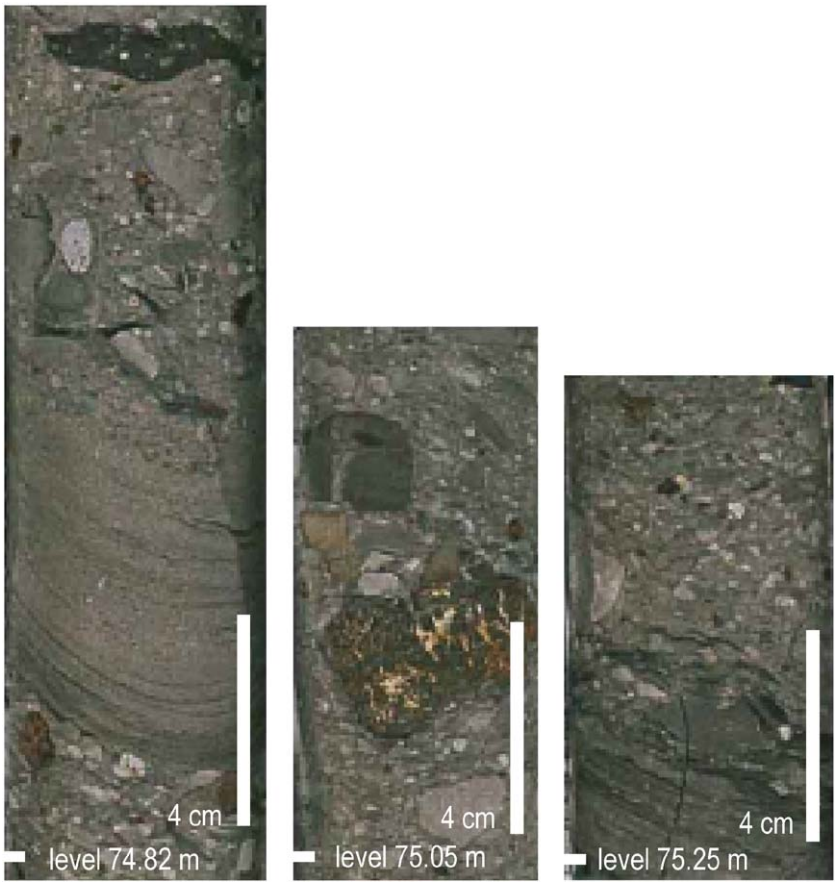

Fig. 9. Details from subunit IIc. The left image shows the cross-bedded unit at level 74.81–74.71 m centre and right images display details of the clast to matrix supported conglomerate bed at level 75.27–74.81.

These water surges must have led to severe and violent erosion of both the crater rim and central high, and the generation of several phases of bypassing tsunami each adding more material to the crater-fill.

In this context, it is interesting that each of the crater-fill subunits IIa, IIb and IIc is lithologically distinct, and is composed of various types of sedimentary rock clasts. This points at least to gradual "unroofing" of the central high by successive stages of erosion. The various clasts of subunits IIa and IIc show lithologies that indicate an origin from rocks and contain both shock metamorphic quartz grains that were crushed by the impact shock waves and Ir-enrichments (Melosh, 1989; Sandbakken, 2002).

3.2.1. Subunit IIa—central high collapse, slope instability

The 5-cm-thick siderite bed (Fig. 5) most likely is a diagenetic alteration product of fine-grained, laminated siltstone. However, we cannot exclude the possibility of an originally pre-impact siderite clast, since siderite concretions are very common diagenetic phases in the pre-impact formations of the Barents Sea. Its bedding is parallel to subunit IIa bedding and is at an angle to the bedding of unit I. Consequently, we consider it as the base of unit II. In either case, a diagenetic formation during reducing and alkaline conditions is indicated with a short break in the sedimentation. The colour zonation of the brown to beige siderite resembles that produced by thermal alteration. Did the heat bake it just after impact?

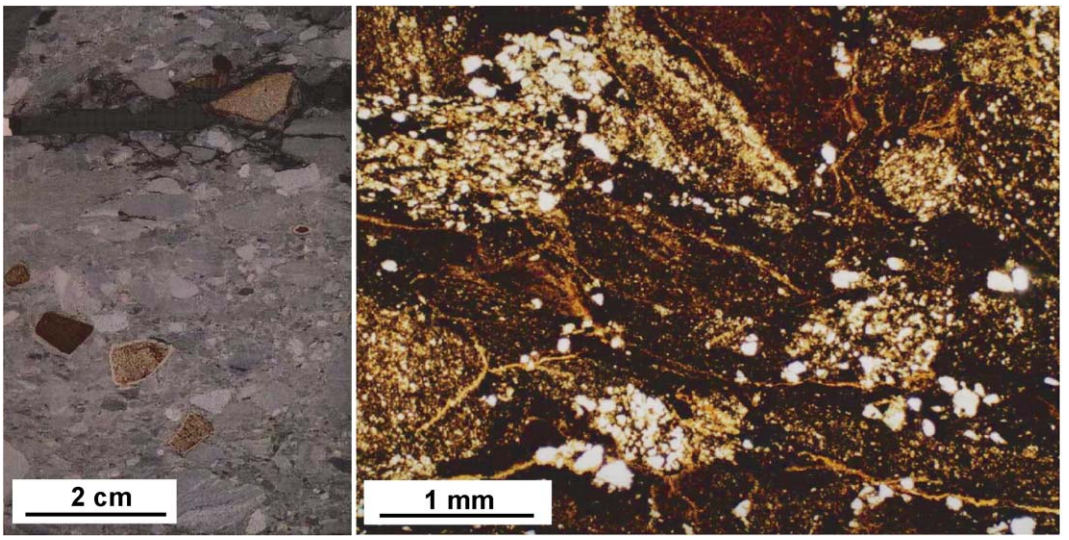

Fig. 10. General impression of the sediments in unit IIc. The left image is a core photo (75.15–75.05 m, split core) showing a light grey conglomerate with a mainly clast-supported texture. Some of the clasts seem to be altered, with a yellowish rim along the edges. The right image shows a thin section micrograph (75.30 m, plane-polarized light) with randomly oriented, dark brown clasts of claystones and mudstones, embedded in a clayey, sand dominated matrix.

The uppermost, finely laminated part of the siderite shows a laminated texture that could indicate deposition from suspension. In contrast, the lower part of the siderite shows septarian developments and calcite fracture fillings that were highly disturbed during early diagenesis.

The generally poor sorting and matrix-supported structure of the succeeding 87 cm diamict of subunit IIa, and its flow-like appearance, together with the sharp contact with the siderite bed, indicate a debris-flow related origin for these deposits. Within the subunit, however, three internal zones are present, separating a structureless and two coarsening upward sequences. The thin mudstone beds in between the coarser-grained units may mark short breaks in the violent en-masse sediment transport or represent internal shear zones within the debris-flow. The orientation of clasts parallel bedding, as occurs in level 87.65 m would favour internal shear zone interpretation (e.g. Postma, 1984). Hence, there are features that are in favour of the argument that the diamict of unit IIa has been deposited as one event, although it can not entirely be excluded at this point that the thin intercalated mudstone beds represent breaks in sedimentation.

The origin of the debris flow event(s) must relate to a still unstable central high associated with an decrease in plasticity and viscosity of the sediment mass due to intake of water. It is possible that at this stage in evolution of the central high liquefaction processes were important and that the liquefaction and subsequent remoulding of the unstable sediment pile that forms the central high may be related to its collapse. On the other hand, tsunami may have contributed to the formation of the diamict, too.

3.2.2. Subunit IIb—central high island, tsunami

The most striking feature of unit IIb mudstone unit is the fining upward in grain size (from 14 to 3 μm median diameter), which point to gradual settling from suspension. If this is true, then it may have taken several days for the bed to deposit. The uppermost 2 m of the subunit contains large numbers of *Tasmanites* algae (often more than 1 mm in diameter) (Fig. 7), which can be explained by the relatively slow settling of the large amorphous and buoyant algal bodies that were suspended during the reworking and transport process. It may also explain the bimodality of the grain size distribution and the coarsening of the mean grain size at the very top.

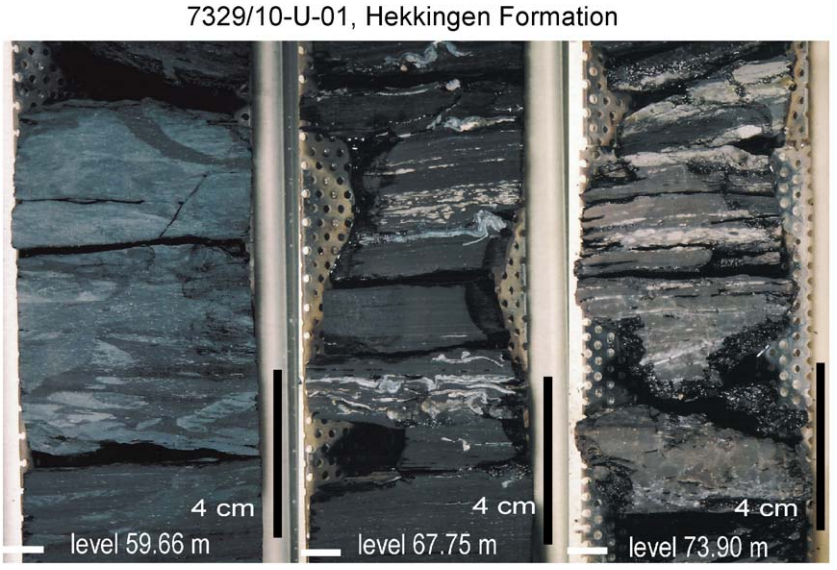

Fig. 11. Photographs of typical Hekkingen Formation. The left image shows grey shales of the upper part of the Hekkingen Formation rich in trace fossils, all representing infaunal elements, which demonstrates "good" living conditions. The centre image displays typical dark grey, organic-rich shales with light grey laminae of fossil fragments of, e.g., *Buchia* and ammonites. The right image shows dark grey shales with conglomeratic zones near level 73.90 m.

A second striking feature of the mudstone unit is the presence of mudstone clasts and breccia, best revealed in thin section, which resemble a diamict fabric. The clasts have, however, similar grain sizes as the neighbouring matrix and some levels in unit IIb display clast-breccia texture in the form of jigsaw

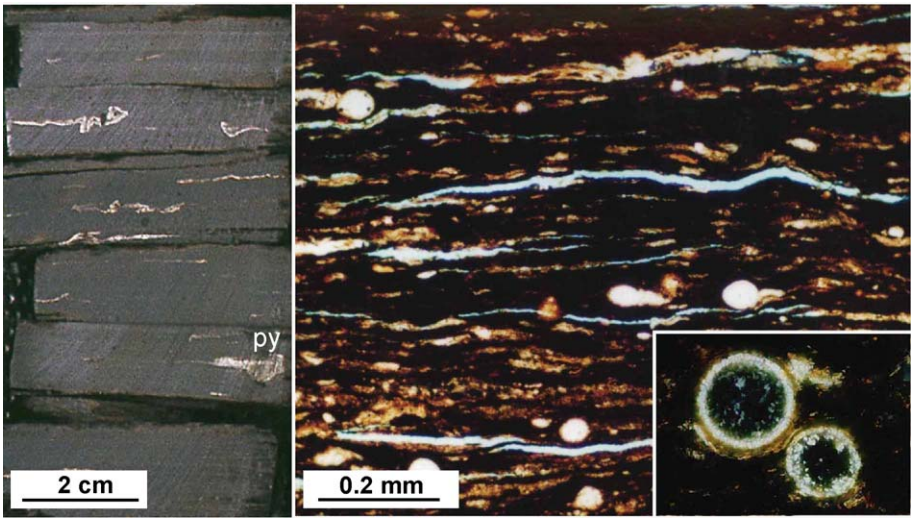

Fig. 12. General views of the Hekkingen Formation. In the left image (core piece 65.36–65.27 m) dark grey, laminated mudstone contains shell fragments oriented parallel to the lamination. A nodule of pyrite is shown in the lower right (py). The right image shows a thin section micrograph (67.10 m, plane-polarized light) with dark and finely laminated shale containing lenses of reddish (organic?) material, and spherical algae seen as white dots. In the lower right image (inset), the same type of algae is shown enlarged (73.70 m, cross-polarized light). These do not correspond to the scale bars, and have diameters of 0.06 and 0.04 mm.

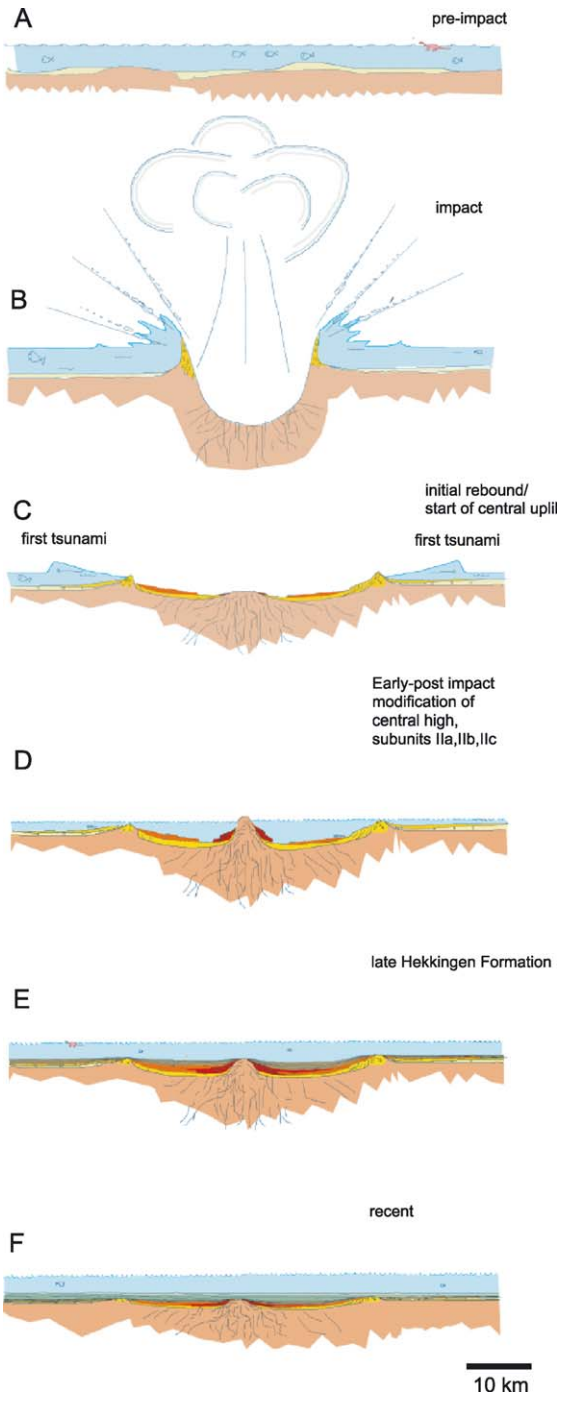

Fig. 13. Conceptual model of the general development of the Mjølnir crater, partly based on Shuvalov et al. (2002) and the present study.

puzzle (as if the fractured parts hardly moved relative to each other, see Fig. 7). The cross-cutting secondary zonation structures in the central parts of subunit IIb may represent fluid escape structures, which are visible due to secondary diagenetic processes. We submit all this as evidence for late- and possibly post-depositional auto-brecciation (cf. Mueller and Cochran, 2001), meaning that there must have been slight and slow (creep) movement of the entire mud mass during and/or just after the phase of suspension settling that we hold responsible for the fining upward sequence. The plastic deformation shown by some of the clasts we ascribe to post-impact burial.

The mineralogical (Sandbakken, 2002) and faunal (Bremer et al., 2003) compositions of the subunit are similar to those of the pre-impact Triassic to Jurassic strata (as seen from Svalbard and areas north in the Barents Sea). Smelror et al. (2001b) recognized palynomorphs in subunit IIb typical of the Jurassic part of the Hekkingen Formation, as present elsewhere in the Barents Sea region.

Subunit IIb is very similar to the homogenites described by Cita et al. (1996) and Takayama et al. (2000), which were inferred to result from tsunami reworking of basin margin sediments. Subunit IIb would represent what Palmer and Neall (1991) called a debris avalanche, before developing into a debris flow. Their example was triggered by pressure differences and erosion created by powerful tsunami. A tsunami that induces dynamic loading on the flanks of the central high might be able to cause a kind of "explosive" liquefaction and subsequent gliding of the liquefied and brecciated mass (due to large pressure differences). The question is whether such processes can explain the jigsaw fabric of breccia clasts and the similarity of grading.

Summarizing: Unit I and subunits IIa and IIb are inferred to represent the entire impact history, where the slided and slumped sediment slabs, represented by unit I, are about time equivalent with the rise of the central high, whereas unit IIa would represent the collapse of the high (abundant liquefaction processes and possibly tsunami); and unit IIb the tsunami-phase and termination of the impact event, before the major modification phase. This sedimentary sequence shows much resemblance with the megabeds described by Kleverlaan (1987) from intermontane basin in SE Spain. The

latter author describes megabeds that were related to seismic events that caused collapsing of the entire margin of a 400–600-m deep basin. The megabeds show a basal unit (I) consisting of gigantic folded clasts (>100 m^3) of original marine substrate bedded in matrix supported conglomerate; a unit II consisting of a complex mixture of debris flow and turbulent flow deposits; a unit III with turbidity current deposits that grade into a unit IV, a graded mudstone unit, both having been related to tsunami. In this case, the tsunami related deposition is much coarser grained and more thickly developed than in our case, probably reflecting different basin configurations.

3.2.3. Subunit IIc—central high island, drowning

The subunit IIc lithologies are interpreted to represent various types of debris-flow deposits and turbidites. These were deposited before the normal "Hekkingen" conditions returned with sedimentation of dark grey, organic-rich clays. The subunit IIc beds contain compacted mud clasts and quartz grains with shock metamorphic features (shocked quartz, Ir-enrichments, see Sandbakken, 2002). The polymict, poorly sorted conglomerates are comparable with those found in other, steep-slope environments like those of coarse grained deltas (Postma and Roep, 1985; Postma et al., 1988; McCaffery and Kneller, 2001). Those authors noticed that debris-flow type deposits often are succeeded by turbidite-type deposits without any preservation of fine-grained tail beds of the turbidites. A similar upward transition from debris-flow bed to turbidite is sharp in this core (e.g. level 74.71–74.31 m, Fig. 8) and similar to that described by Postma et al. (1988) and Sohn (2000).

The thin, polymict and polymodal conglomerate beds of subunit IIc were most likely deposited during several subsequent sediment gravity flows. Their mineralogical composition is relatively similar (Sandbakken, 2002), except for variations in clay mineral composition (smectite/chlorite and kaolinite) and a relatively large increase in the amount of plagioclase in the upper part (Dypvik et al., 2003).

The number of beds suggests that subunit IIc spans a significant time period reflecting the gradual reworking of the flanks of the central during its subsequent drowning (Fig. 13).

3.3. Hekkingen Formation

A final return to normal marine depositional conditions of the region is reflected in the 16-m-thick Late Volgian-Ryazanian Hekkingen Formation and the succeeding 7-m-thick Valanginian to Hauterivian Klippfisk Formation overlying subunit IIc (Smelror et al., 2001b). The Hekkingen Formation is here represented by the Krill Member (Worsley et al., 1988), which constitutes the upper part of the formation. The mudstones are well laminated, containing abundant bivalves (*Buchia*) and ammonites. The mudstones were deposited in partly anoxic to hypoxic shelf environments, with a good preservation potential for organic matter.

At level 74.05 m in our core, the occurrence of dark grey mudstones typical for the Hekkingen Formation indicate the return to hypoxic depositional conditions, which dominated the area a few million years before and after the impact. The depositional conditions were dominated by highly productive waters, enriched in organic matter and skeletal fragments (Bremer et al., 2003; Smelror et al., 2001a,b). High clastic accumulation rates, parallel lamination and high organic content illustrate the lack of bioturbation and the good preservation of organic matter. By this time, the most dramatic relief of the crater had been levelled, as is evident from the return of more low energy sedimentation conditions in the basin, as dominated in the region before impact (Leith et al., 1993).

The zone from 73.89 to 73.78 m, where several thin conglomeratic beds appear (Figs. 8, 9 and 11), reflects the last coarse-grained sedimentation of reworked impact-related material in this core, possibly sourced from a few remaining, high-relief localities. There, debris flows and turbidity currents transported clastic material, including different clasts and rip-up clasts, into central parts of the basin, possibly during storm events that reworked the shoals formed by the inferred high-relief localities. The uppermost five of the six conglomeratic layers present in the Hekkingen Formation have a polymict clast composition, different from the surrounding mudstone. It is important to note that the 5-cm-thick, lowermost layer of these units consists almost entirely of rip-up clasts of the Hekkingen Formation. It shows that newly deposited, partly consolidated

Hekkingen Formation was eroded, perhaps in connection with local tectonic disturbances related to the central high, and deposited as scree and slides along its sides (Fig. 13).

The five 1–2-cm-thick conglomeratic layers following just above the 5-cm layer of rip-up clasts have a composition showing erosion of material similar to the ones forming the conglomerates of the Ragnarok Formation (especially subunit IIc) below. This sudden reappearance of the light grey clay and siltstone clasts may imply that the central high was still subject to some erosion. The lack of signs of oxidation indicates that the high at this stage most likely was covered by sea and formed a shallow submarine bar, as probably did the crater rim during this post-impact phase sedimentation in the paleo-Barents Sea.

Towards the top of the Hekkingen Formation (68–57.10 m), more ventilated depositional conditions are seen (Fig. 13). This is reflected in the lighter grey shales, and in the gradual transition to the light, greenish grey marls and limestones of the Klippfisk Formation. Bioturbation is also abundant in these youngest of the Hekkingen sediments, dominated by infauna, showing that oxic conditions were developing within the sediments.

At the end of the Jurassic, the Mjølnir impact (142 ± 2.6), the Morokweng (South Africa, 145.0 ± 0.8 Ma; Hart et al., 1997; Koeberl et al., 1997) and the Gosses Bluff (Australia, 142.5 ± 0.8 Ma; Crook and Cook, 1966; Milton et al., 1996) took place. According to the global impact database, five additional impacts may have happened at about the same time (http://www.unb.ca/passc/ImpactDatabase/). But so far, none of these seven impacts have been proven to be of submarine origin. Therefore, we will just give some few comparative statements with the Mjølnir impact crater and the submarine Montagnais impact crater (50.5 ± 0.76Ma; Jansa et al., 1989) here and refer to Dypvik and Jansa (2003) for further comparison.

Both the Mjølnir and the Montagnais craters had elevated rims and uplifted high central highs controlling the crater fill sedimentation. While some melt rocks have been found in the Montagnais crater sediments, so far these are missing in the sediments from the Mjølnir impact crater. Otherwise, both crater-fill sequences seem to be dominated by reworking and resedimentation from older formations, and the processes of density and gravity flows, slumps and avalanches are of outmost importance, together with an intense tsunami activity.

4. Conclusions

The sediments deposited along the central high of the Mjølnir crater were studied in a 121-m long core showing deposition from the time of uplift of the central high to its complete stabilization (Fig. 13). From a detailed sedimentological study of the core, we tentatively conclude:

(1) that large sediment slabs of the original sea-floor slided and slumped into the crater during the rising of the central high;
(2) that diamict of unit IIa is related to the collapse phase of the central high producing liquefaction and causing remoulding and flow of watery sediment masses, leaving open the possibility that the debris flows are related to tsunami;
(3) that the in situ brecciated graded mudstone unit represents the last phase of the impact possibly showing the effects of tsunami waves and settling of the sediment from suspension. At this time, the crater was submerged by the sea once more;
(4) the succeeding coarse grained turbidite unit deposited just below the Hekkingen Formation represents the final drowning of the central high;
(5) the organic-rich mudstones of the Hekkingen Formation point to full reestablishment of pre-impact marine conditions;
(6) that the sequence of events found in the Mjølnir crater so far justify the numerical modelling results of Shuvalov et al. (2002).

Acknowledgements

We thank M. Smelror and J.O. Vigran for the palynological dating; P. Sandbakken and F. Langenhorst for their work on the shock metamorphism of core sediment. G.M.A. Bremer is thanked for several discussions on the micropaleontology of the successions and Ø. How for excellent help in the core lab. The project was financially supported by The

Research Council of Norway (NFR). The comments of referees K.A.W. Crook, C.W. Poag and R. Cas on an earlier draft are highly appreciated.

References

Bremer, G.M., Smelror, M., Nagy, J., Vigran, J.O., 2003. Biotic responses to the Mjølnir meteorite impact, Barents Sea: evidence from a core drilled within the crater. ESF Impact Program, Proceedings, Svalbard Meeting 2001. 21–38 pp.

Cita, M.B., Camerlenghi, A., Rimoldi, B., 1996. Deep-sea tsunami deposits in the eastern Mediterranean: new evidence and depositional models. Sediment. Geol. 104, 155–173.

Crook, K.A.W., Cook, P.J., 1966. Gosses Bluff-diaper, crypto-volcanic structure or astrobleme? J. Geol. Soc. Aust. 13, 495–516.

Dypvik, H., Jansa, L., 2003. Sedimentary signatures and processes during marine bolide impacts: a review. Sediment. Geol. 161, 309–337.

Dypvik, H., Gudlaugsson, S.T., Tsikalas Jr., F., Attrep Jr., M., Ferrell, R.E., Krinsley, D.H., Mørk, A., Faleide, J.I., Nagy, J., 1996. Mjølnir structure: an impact crater in the Barents Sea. Geology 24, 779–782.

Dypvik, H., Kyte, F., Smelror, M., 2000. Iridium peaks and algal blooms. The Mjølnir Impact. Abstr. 31st. Lunar and Planetary Science Conference, Houston, Texas, March 13–17.

Dypvik, H., Ferrell, R.E., Sandbakken, P.T., 2003. The clay mineralogy of sediments related to the marine Mjølnir impact crater. Meteorit. Planet. Sci. 38, 1–14.

Dypvik, H., Mørk, A., Sandbakken, P., Smelror, M., Vigran, J.O., Bremer, G.M.A., in press. The Ragnarok Formation and Sindre Bed of the Arctic. Nor. Geol. Tidsskr.

French, B.M., 1998. Traces of catastrophe: a handbook of shock-metamorphic effects in terrestrial meteorite impact structures. LPI Contribution, vol. 954. Lunar and Planetary Institute, Houston, USA. 120 pp.

Gudlaugsson, S.T., 1993. Large impact crater in the Barents Sea. Geology 21, 291–294.

Hart, R.J., Andreoli, M.A.G., Redoux, M., Moser, D., Ashwal, L., Eide, E., Webb, S.J., Brandt, D., 1997. Late Jurassic age for the Morokweng impact structure, southern Africa. Earth Planet. Sci. Lett. 147, 25–35.

Jansa, L.F., Pe-Piper, G., Robertson, B.P., Friedenreich, O., 1989. Montagnais: a submarine impact structure on the Scotian shelf, eastern Canada. Geol. Soc. Amer. Bull. 101, 450–463.

Kleverlaan, K., 1987. Gordo Megabed: a possible seismite in a Tortonian submarine fan: Tabernas Basin, Province Almeria, Southeast Spain. Sediment. Geol. 51, 165–180.

Koeberl, C., Armstrong, R.A., Reimold, W.U., 1997. Morokweng, South Africa; a large impact structure of Jurassic–Cretaceous boundary age. Geology 25, 731–734.

Leith, T.L., Weiss, H.M., Mørk, A., Århus, N., Elvebakk, G., Embry, A.F., Brooks, P.W., Stewart, K.R., Pchelina, T.M., Bro, E.G., Verba, M.L., Danyushevskaya, A., Borisov, A.V., 1993. Mesozoic hydrocarbon source-rocks of the Arctic region. In: Vorren, T.O., Bergsager, E., Dahl-Stammers, O.A., Holter, E., Johansen, B., Lie, E., Lund, T.B. (Eds.), Arctic Geology and Petroleum Potential. NPF Special Publication, vol. 2. Elsevier, pp. 1–25.

Lindstrøm, M., Sturkell, E.F.F., Tørnberg, R., Ormø, J., 1996. The marine impact crater at Lockne, Central Sweden. Geol. Føren. Stockh. Förh. 118, 193–206.

McCaffery, M., Kneller, B., 2001. Process controls on the development of stratigraphic trap potential on the margins of confined turbidite systems and aids to reservoir evaluation. AAPG Bull. 85, 971–988.

Melosh, H. J., 1989. Impact Cratering: A Geologic Process, 245 pp., Oxford Univ. Press, N.Y. and Clarendon Press, Oxford.

Milton, D.J., Glikson, A.Y., Brett, R., 1996. Gosses bluff; a latest Jurassic impact structure, Central Australia: part 1. geological structure, stratigraphy, and origin. In: Glikson, A.Y. (Ed.), Australian Impact Structures. AGSO Journal of Australian Geology and Geophysics. vol. 16, pp. 453–486.

Mueller, W.U., Cochran, P.L., 2001. Volcano-sedimentary processes operating on a marginal continental arc: the Archean Raquette Lake Formation, Slave Province, Canada. Sediment. Geol. 141–142, 169–204.

Palmer, B.A., Neall, V.E., 1991. Contrasting lithofacies architecture in ring-plain deposits related to edifice construction and destruction, the quaternary stratford and opunake formations, Egmont Volcano, New Zealand. Sediment. Geol. 74, 71–88.

Poag, C.W., Plescia, J.B., Molzer, P.C., 2002. Ancient impact structures on modern continental shelves: the Chesapeake Bay, Montagnais, and Toms Canyon Craters, Atlantic margin of North America. Deep-Sea Res., Part 2, Top. Stud. Oceanogr. 49, 1081–1102.

Poag, C.W., Koeberl, C., Reimold, W.U., 2003. The Chesapeake Bay Crater: Geology and Geophysics of a Late Eocene Submarine Impact Structure. Springer-Verlag, Heidelberg. 522 pp.

Postma, G., 1984. Mass-flow conglomerates in a submarine canyon: Abrioja Fan-delta, Pliocene, SE Spain. In: Koster, E.H., Steel, R.J. (Eds.), Sedimentology of Gravels and Conglomerates. Can. Soc. Petrol. Geol. Mem., vol. 10, pp. 237–258.

Postma, G., Roep, Th.B., 1985. Resedimented conglomerates in the bottomset of a Gilbert-type gravel delta. J. Sediment. Petrol. 55, 874–885.

Postma, G., Nemec, W., Kleinspehn, K.L., 1988. Large floating clasts in turbidites: a mechanism for their emplacement. Sediment. Geol. 58, 47–61.

Sandbakken, P.T., 2002. A geological investigation of the Mjølnir crater core (7329/03-U-01), with emphasis on shock metamorphosed quartz. Cand Scient Thesis, Univ. of Oslo. 142 pp.

Shuvalov, V.V., Dypvik, H., Tsikalas, F., 2002. Numerical simulations of the Mjølnir marine impact crater. J. Geophys. Res. 107 (10.1029/2001JE001698, 1-1-1-13).

Shuvalov,V., Dypvik, H., in press. Ejecta formation and crater development of the Mjølnir impact. Meteoritics and Planetary Geology.

Smelror, M., Mørk, A., Monteil, E., Rutledge, D., Leereveld, H., 1998. The Klippfisk Formation a new lithostratigraphic unit of Lower Cretaceous platform carbonates on the Western Barents Shelf. Polar Res. 17 (2), 181–202.

Smelror, M., Kelly, S.R.A, Dypvik, H., Mørk, A., Nagy, J., Tsikalas, F., 2001a. Mjølnir (Barents Sea) meteorite impact ejecta offers a Volgian-Ryazanian boundary marker. Newsl. Stratigr. 46 (2/3), 129–140.

Smelror, M., Dypvik, H., Mørk, A., 2001b. Phytoplankton blooms in the Jurassic–Cretaceous boundary beds of the Barents Sea possibly induced by the Mjølnir Impact. In: Buffetaut, E., Koeberl, C. (Eds.), Geological and Biological Effects of Impact Events. Impact Studies Springer, Heidelberg, pp. 69–81.

Sohn, Y.K., 2000. Coarse-grained debris-flow deposits in the Miocene fan deltas, SE Korea: a scaling analysis. Sediment. Geol. 130, 45–64.

Takayama, H., Tada, R., Matsui, T., Iturralde-Vinent, M.A., Oji, T., Tajika, E., Kiyokawa, S., Garcia, D., Okada, H., Hasegawa, T., Toyda, K., 2000. Origin of the Peñalvar Formation in northwestern Cuba and its relation to K/T boundary impact event. Sediment. Geol. 135, 295–320.

Tsikalas, F., Gudlaugsson, S.T., Eldholm, O., Faleide, J.I., 1998a. Integrated geophysical analysis supporting the impact origin of the Mjølnir Structure, Barents Sea. Tectonophysics 289, 257–280.

Tsikalas, F., Gudlaugsson, S.T., Faleide, J.I., 1998b. Collapse, infilling, and postimpact deformation at the Mjølnir impact crater, Barents Sea. Geol. Soc. Amer. Bull. 110, 537–552.

Tsikalas, F., Gudlaugsson, S.T., Faleide, J.I., 1998c. The anatomy of a buried complex impact structure: the Mjølnir structure, Barents Sea. J. Geophys. Res. 103, 30469–30484.

Vigran, J.O., Mangerud, G., Mørk, A., Bugge, T., Weitschat, W., 1998. Biostratigraphy and sequence stratigraphy of the Lower and Middle Triassic deposits from the Svalis Dome, central Barents Sea, Norway. Palynology 22, 89–141.

Von Dalwigk, I., Ormø, J., 2001. Formation of resurge gullies at impacts at sea; the Lockne crater, Sweden. Meteorit. Planet. Sci. 36, 359–369.

Worsley, D., Johansen, R., Kristensen, S.E., 1988. The Mesozoic and Cenozoic succession of Troms Flaket. In: Dalland, A., Worsley, D., Ofstad, K. (Eds.), A Lithostratigraphic Scheme for the Mesozoic and Cenozoic Succession Offshore Mid- and Northern Norway. Nor. Pet. Direct., vol. 4. 65 pp.

Zakharov, V.A., Lapukhov, A.S., Shenfil, O.V., 1993. Iridium anomaly at the Jurassic–Cretaceous boundary in northern Siberia. Russ. J. Geol. Geophys. 34, 83–90.